ACS ES&T Air

pubs.acs.org/estair
Article

Molecular Characterization and Photoreactivity of Organic Aerosols Formed from Pyrolysis of Urban Materials during Fires at the Wildland–Urban Interface

Published as part of ACS ES&T Air special issue "Wildland Fires: Emissions, Chemistry, Contamination, Climate, and Human Health".

Katherine S. Hopstock, Qiaorong Xie, Michael A. Alvarado, Vaios Moschos, Solomon Bililign, Jason D. Surratt, Alexander Laskin, and Sergey A. Nizkorodov*

Cite This: ACS EST Air 2024, 1, 1495–1506
Read Online

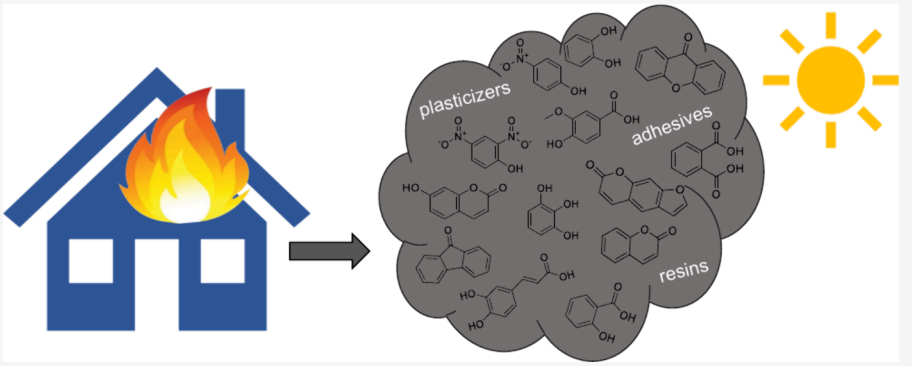

ABSTRACT: Fires at the wildland–urban interface (WUI) are increasing in magnitude and frequency, emitting organic aerosol (OA) with unknown composition and atmospheric impacts. In this study, we investigated the chemical composition of OA produced through the 600 °C pyrolysis of ten urban materials in nitrogen, which were subsequently aged under UV light for 2 h. The analysis utilized ultrahigh-performance liquid chromatography (UHPLC) separation, coupled with a photodiode array (PDA) detector and a high-resolution mass spectrometer (HRMS) for molecular characterization. Hierarchical clustering analysis demonstrated that lumber-derived OA was the most diverse and distinct in composition. Unaged and aged OA (for each urban material) did not significantly differ in chemical identities. Potential aromatic brown carbon (BrC) chromophores (based on their degree of unsaturation) constituted 13–42% of all assigned compounds. PDA chromatograms revealed multiple BrC chromophoric species that were either enhanced or degraded as a result of UV aging, providing insights into specific BrC chromophores responsible for photobleaching and photoenhancement of the overall absorption coefficient. Thirty-six BrC chromophores were identified across the ten OA types, and their structures were confirmed using reference standards. Components of plasticizers and resins, such as phthalic and terephthalic acids, were structurally confirmed in the samples. We present potential species for WUI fires as components of resins, epoxies, dyes, and adhesives commonly used in manufacturing urban materials. Photolysis did not significantly impact the chemical composition of OA emitted from the burning of specific WUI materials.

KEYWORDS: *pyrolysis, construction materials, organic aerosol, brown carbon, chromophores, UV aging, high-resolution mass spectrometry, wildland–urban interface*

INTRODUCTION

The wildland-urban interface, or WUI, is defined as the area where structures and other human developments meet or intermingle with wildland vegetation.[1,2] In 2010, the US Forest Service estimated that 43.4 million new homes were in WUI communities, making WUI areas the fastest-growing land use type in the contiguous US.[3] The increasing frequency of large-scale forest fires raises the risk of fire encroachment into the WUI.[4,5] These devastating events can begin with wildfire

Received: August 23, 2024
Revised: October 7, 2024
Accepted: October 9, 2024
Published: October 17, 2024

flames directly passing into urban spaces or with embers spreading to urban structures, initiating smoldering combustion that can ultimately develop into flaming combustion.[6−9] The burning of engineered construction materials can lead to atmospheric emissions not typically found in wildland fires and are poorly characterized. As global models routinely underpredict the formation, mass loadings, and temporal trends of anthropogenic organic aerosol (OA), insights into the chemical composition and atmospheric transformations of particulate matter (PM) emitted from WUI fires can help reduce these uncertainties.[10,11]

The fuels primarily burned in WUI fires are those used in and around residential homes, commercial buildings, and other relevant structures. A typical residential house in the United States is constructed, on average, from ∼97% wood and ∼2% asphalt shingles (by weight), whereas its interior contents range from ∼40−90% wood, ∼12−26% plastic, and ∼0−20% fabric.[1] Common building materials include insulation (made from polyurethane, polyisocyanurate, glass wool, and phenolic foams), vinyl siding, polyvinyl chloride (PVC) windows, upholstery on furniture, vinyl and polyamide carpets, electrical wiring insulation (typically PVC), acrylic clothing, and furniture.[12−14] Although these materials are vastly different from biomass, they undergo similar thermal decomposition stages, emitting both PM and volatile organic compounds (VOCs).[12] During the combustion of traditional wooden materials, polycyclic aromatic hydrocarbons (PAHs) and their derivatives can be emitted, which contribute to light absorption by aerosol particles, thus impacting air quality and climate.[15,16] Chemically treated wooden materials are common in WUI spaces, but their combustion emission characteristics are unknown. The combustion of PVC and other plastics is known to emit halogenated organics, such as polychlorinated dibenzodioxins and polychlorinated dibenzofurans, which are toxic.[17,18] Emissions of halogenated organics lead to significant increases in atmospheric concentrations of chlorine and hydroxyl radicals ($Cl^{\bullet}$ and $^{\bullet}OH$, respectively). Attention has been drawn to plastic burning, as halogen-containing aerosols can have climate implications; however, organic emissions from these materials have been understudied, and their impacts remain unclear.[1,19] Additionally, in terms of human health, WUI fires pose a great risk to PM and VOC exposure because of their proximity to residential communities and first responders at the scene.

Studies have examined the emissions, transportation, and aging processes of OA produced during the combustion of biomass fuels in regions such as Western North America, Siberia, Amazonia, and Central Africa.[20−28] The pyrolysis of biomass, which contains biopolymers like lignin, cellulose, and hemicellulose, is well understood to produce phenolic compounds (such as catechol, guaiacol, and coniferaldehyde), organic acids (like benzoic acid and salicylic acid), furans, coumarins, flavonoids, and stilbenes. Some of these compounds are light-absorbing, leading to a classification of pyrolysis OA as brown carbon (BrC).[29−32] Nitrogen-containing aromatic compounds (NACs), specifically nitrophenols (such as 4-nitrocatechol and 2,4-dinitrophenol) strongly absorb UV and visible radiation and are common BrC chromophores in biomass burning organic aerosol (BBOA).[33−42]

BrC compounds are known to undergo photochemical transformations during atmospheric transport, exhibiting both photoenhancement and photobleaching behaviors.[35,36,43−45] Certain physicochemical properties, such as molecular weight, structural composition, volatility, and oxidation state, have been shown to correlate with BrC absorption characteristics and stability with respect to UV exposure.[30,46−48] For example, Di Lorenzo et al. examined BBOA field samples and found that higher molecular weight chromophores (>500 Da) exhibited the majority of absorption, while smaller molecular weight fractions were more susceptible to photobleaching degradation.[49] Calderon-Arrieta et al. examined the change in BrC bulk absorption as a function of thermal evaporation of volatile components.[50] Upon evaporation, samples darkened, and molecular characterization demonstrated that small, oxygenated, less-absorbing monoaromatic compounds were depleted, whereas large and less polar substituents remained.[50] Neither the physiochemical properties nor the molecular evolution as a function of UV exposure are well understood for OA produced through the combustion of urban construction materials, thus prompting this pilot study.[1]

Previously, we found that OA from pyrolyzed urban materials exhibited distinct optical absorption properties, each responding differently to photolytic aging.[51] Of the ten different types of investigated OA, two photobleached, two remained unchanged, and six underwent photoenhancement after 2 h of UV exposure.[51] The goal of this study is to investigate the molecular composition of OA in both unaged and photochemically aged samples from Hopstock et al.[51] Additionally, our goal is to identify both common and unique BrC chromophores responsible for absorption in each pyrolyzed urban material and to propose potential compounds characteristic of emissions from the WUI. Our approach relies on ultrahigh-performance liquid chromatography (UHPLC) separation, coupled with a photodiode array (PDA) detector and a high-resolution mass spectrometer (HRMS) for molecular characterization. This investigation provides molecular insights into the light absorption properties of PM emissions from WUI fires and, for the first time, explains how OA molecular composition transforms during atmospherically relevant photolytic exposure.

METHODS

Ten urban materials in Hopstock et al. were selected to represent common structural and furnishing components burned in WUI fires.[51] These include carpet, electrical 23 AWG wire (with purple PVC coating, referred to as "thin PVC wire"), vinyl flooring, synthetic fabric, plywood, ceiling tile, electrical 12 AWG wire (with white PVC coating, referred to as "thick PVC wire"), drywall, fiberboard, and lumber. As described in Hopstock et al.[51] and in SI Appendix A, the urban materials were pyrolyzed in a tube furnace at 600 °C under a flow of dry N_2. All OA samples analyzed in the present study were also the subject of the optical classification paper by Hopstock et al.[51] Samples that underwent 2 h of photolysis will be referred to as "aged" from here on out. SI Appendix A provides details on the generation of OA, UHPLC-PDA-HRMS sample preparation, and HRMS analysis.

BrC Standards. A one hundred component BrC standard mixture was obtained from North Carolina A&T State University and the University of North Carolina, Chapel Hill, and was used to verify BrC structural assignments in the OA UHPLC-PDA-HRMS results. This standard mixture was described in detail by Moschos et al.[27] Briefly, CHO and CHON species were selected for the mixture as they are known to be BrC species emitted during biomass burning

https://doi.org/10.1021/acsestair.4c00215
ACS EST Air 2024, 1, 1495−1506

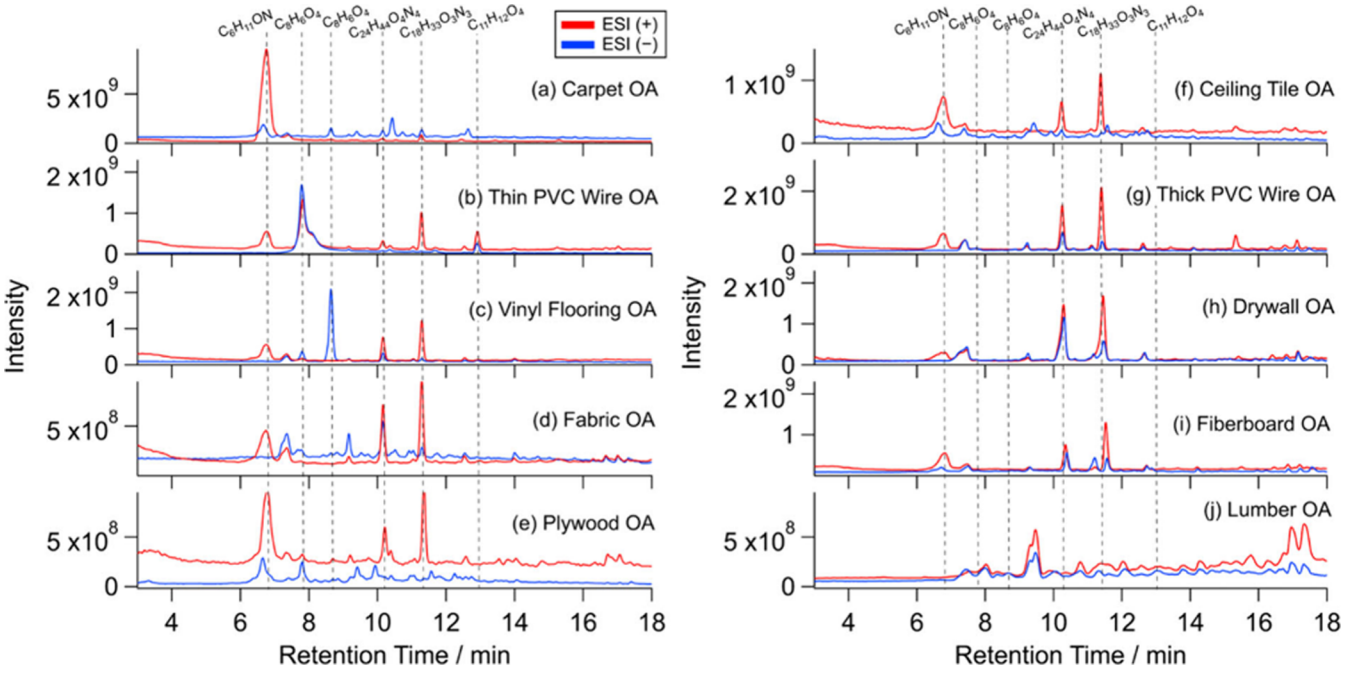

Figure 1. UHPLC-ESI total ion chromatograms collected in the *positive* (red) and *negative* (blue) ionization modes for the ten unaged OA samples (panels a–j). Repeated peaks are indicated by dashed lines and labeled with the major ion's assigned neutral molecular formula.

events. The individual BrC components were initially dissolved in methanol and diluted with water (Optima LC/MS grade, Fisher Chemical) before UHPLC-PDA-HRMS analysis. The final concentration of the combined 100 species solution was 0.3 mg mL^{-1}. The injection volume, LC gradient, ionization parameters, and MS settings were the same as for the OA samples described SI Appendix A. The standard mixture was run with ESI in both ionization modes. Consistent with the report by Moschos et al., our results exhibited distinct retention times for structural isomers due to polarity differences.[27]

Compound Discover and mzVault Library Integration. Compound Discover 3.3.200 SP3 (Thermo Fisher Scientific Inc.) relied on both custom-built and online libraries for processing and interpretation of unknown data. The prebuilt workflow template, "Environmental w Stats Unknown ID w Online and Local Database Searches" was modified to suit the needs of our study. A customized mzVault 2.0 (Thermo Fisher Scientific Inc.) library was manually created by uploading MS^2 spectra (recorded specifically for this study) for each observable compound in the mixture of BrC standards. This library was imported into Compound Discover using the "Search mzVault" node. When cross referencing each OA sample with the mzVault library, Compound Discover was set to use the following parameters: match ion activation type, match ion activation energy, precursor mass tolerance of 5 ppm, and retention time tolerance of 0.2 min to accommodate drifts in LC retention time among samples and BrC standard runs. Table S1 displays the BrC standard species identified with our analytical platform, along with the OA sample in each BrC species identified. Species identified in this manner will be referred to as *structurally identified species* from here on out.

To provide more insight into these OA samples, Compound Discover was set to search mzCloud (mass spectral fragmentation library) and then correlate results with mzLogic. This data analysis algorithm helped fill in the gaps by providing possible candidates for unknown species when a species was not identified with the customized mzVault library. Additionally, the workflow allowed a search of the ChemSpider database to find more potential compound identities. Species identified in this manner, with proposed molecular structures, will be referred to as *tentatively assigned species* from here on out (Table S2). Compound Discover's statistical tools were also deployed in our analysis.

RESULTS AND DISCUSSION

Overall Characteristics of Urban Material OA. Figure 1 presents the total ion chromatograms (TICs) for all OAs collected in the positive (red traces) and negative (blue traces) ionization modes. A few large peaks stood out in the TICs, for example: the $C_6H_{11}ON$ peak (6.76 min) present in ESI(+) for all urban material OA (except lumber); the $C_8H_6O_4$ peak (7.80 min) largely present in ESI(±) for thin PVC wire OA; the $C_8H_6O_4$ peak (8.64 min) in ESI(−) for vinyl flooring OA, identified as terephthalic acid; the $C_{24}H_{44}O_4N_4$ peak (10.16 min) in ESI(+) for all OA except carpet and lumber; the $C_{18}H_{33}O_3N_3$ peak (11.29 min) in ESI(+) for all OA except carpet, fiberboard, and lumber, and the $C_{11}H_{12}O_4$ peak (12.90 min) in ESI (±) for thin PVC wire, ceiling tile, and lumber OA. Several smaller peaks were also present in chromatograms, often merging into unresolved "lumps" of peaks. As the positive ion mode TIC intensities were greater than those in the negative mode, Figures S1 and S2 present the chromatograms separately. The complexity of the TICs, especially evident in Figure S2, necessitated the use of peak deconvolution software (MZmine and Compound Discover) to explore features in greater depth.

As the TICs were comprised of many peaks, including isomeric species with coelution, we started with a broad comparison of OA using the Compound Discover software. This tool allowed us to perform statistical comparisons as shown in the ESI(+) hierarchical clustering in Figure 2 and ESI(±) principal component analyses (PCA) in Figure S3.

https://doi.org/10.1021/acsestair.4c00215
ACS EST Air 2024, 1, 1495−1506

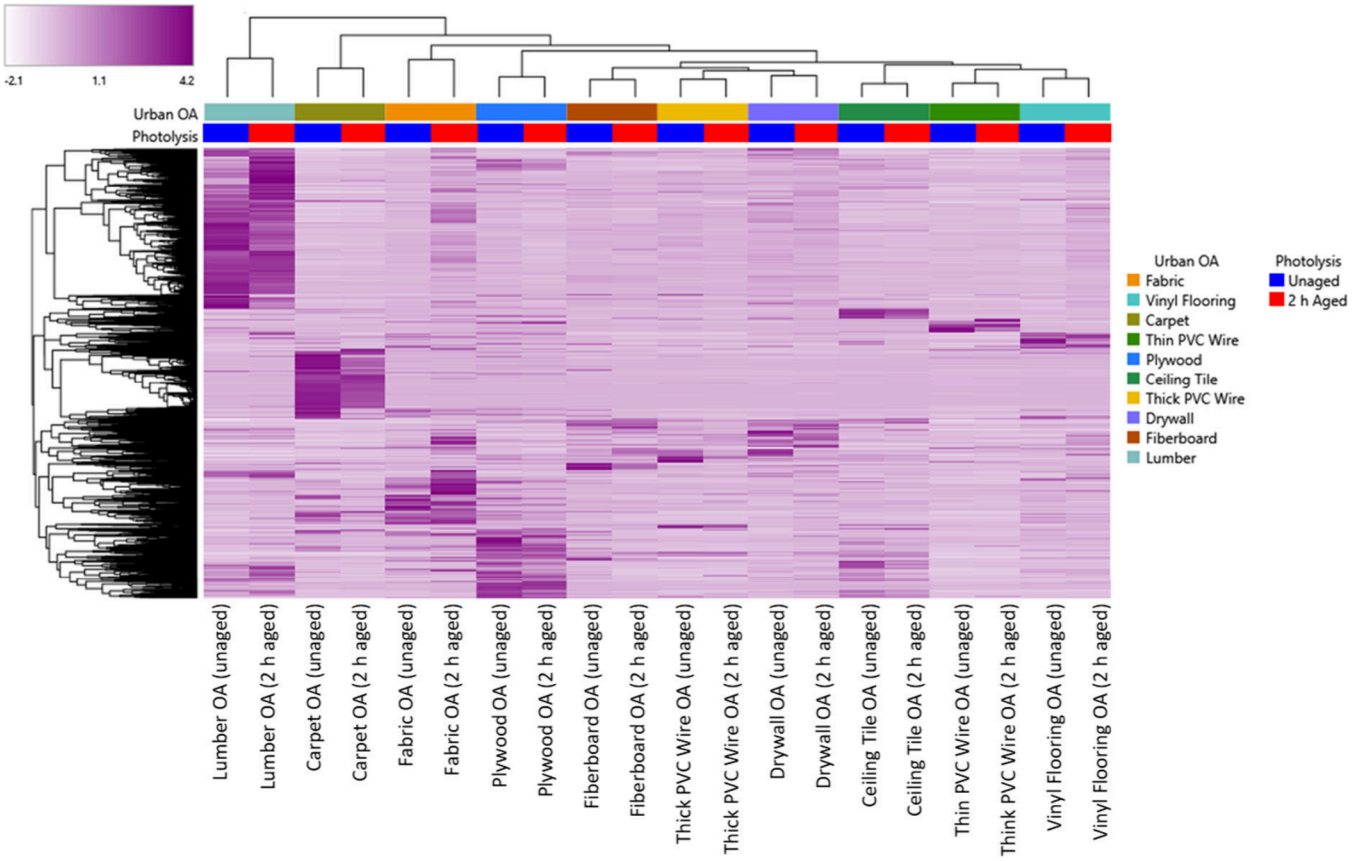

Figure 2. Hierarchical clustering of ESI(+) mass spectral species deconvoluted and identified using Compound Discover 3.3.200 SP3 software (Thermo Fisher Scientific). Columns represent unaged (blue) and aged (red) OA samples. Rows denote individual compounds (assigned with CH, CHO, and CHON molecular formulas) and are scaled using unit variance. The total number of rows (or compounds) detected across all 20 samples was 6509. The distance between clusters (top and left) is based on the correlation distance and average linkage for both rows and columns. The color gradient, ranging from white to purple, represents the abundance of each compound. Standardized matrix values, as determined by the Compound Discover program, were used to scale the data to ensure that all ions have the same range and importance in the color scale.

Each horizontal line in Figure 2 represents a compound detected by the software in at least one of the OA samples, with darker purple colors indicating the highest normalized intensity across all 20 sample/ionization mode combinations. Lumber OA (both unaged and aged) exhibited the greatest number of peaks, which were clustered together furthest away from other OA types. This clustering behavior of lumber OA was also evident in the PCA plots for both ionization modes in Figure S3, indicating that this sample type was the most statistically distinct from the other urban materials. Although lumber and plywood were the two OA types expected to resemble BBOA and each other most closely, they showed minor correlations. This suggests that wooden materials at the WUI may produce OA that is more influenced by synthetic additives rather than traditional biomass/wooden components. OA from more synthetic materials (ceiling tile, thin PVC wire, and vinyl flooring) showed the fewest peaks but resembled each other in their convolution patterns. Overall, Figure 2 and Figure S3 suggested that the unaged and aged OA (for each urban material) were not significantly different in chemical identities. However, when comparing OA types, there was little overlap in chemical identities across the rows in Figure 2. As shown in both panels of Figure S3, unaged and aged OA were most similar for fiberboard, thick PVC wire, thin PVC wire, and vinyl flooring.

Effects of UV Aging on Light Absorbing Species. UHPLC-PDA chromatograms showcased the photobleaching and photoenhancement classifications previously made for these OA samples.[51] In Figure 3 (panels a and b), carpet OA exhibited a reduction in absorbance after UV aging for benzoic acid ($C_7H_6O_2$, the most intense chromophore in the near-UV range), $C_{12}H_{22}ON_2$ (13.3 min), and $C_{16}H_{22}O_4$, $C_{16}H_{31}ON$, $C_{18}H_{33}ON$, and $C_{16}H_{33}ON$ (20−24 min). However, fiberboard OA (Figure 3**c,d**) exhibited the opposite trend. Though major confirmed species (catechol and terephthalic acid) decreased in maximum absorbance, the relative intensity of overall absorbance of all peaks throughout the run increased from 20% (Figure 3c) to 40−80% (Figure 3d) after UV aging. 2D UHPLC-PDA chromatograms exhibiting photobleaching and photoenhancement (for thin PVC wire OA and lumber OA, respectively) are included in Figure S4. For thin PVC wire OA, the two largest UHPLC-PDA features, attributed to phthalic acid and its structural isomer, exhibited a reduction in absorbance between 300 and 400 nm after photolytic aging (red dashed line, Figure S4b). On the contrary, absorbance in the lumber OA (Figure S 4d) sample increased by a factor of 2 between 300 and 400 nm after aging, particularly toward the end of the LC run when more nonpolar species were eluted. Both thin PVC wire and lumber OA weakly absorbed light in the visible wavelength range (Figure S4a,c).

https://doi.org/10.1021/acsestair.4c00215
ACS EST Air 2024, 1, 1495−1506

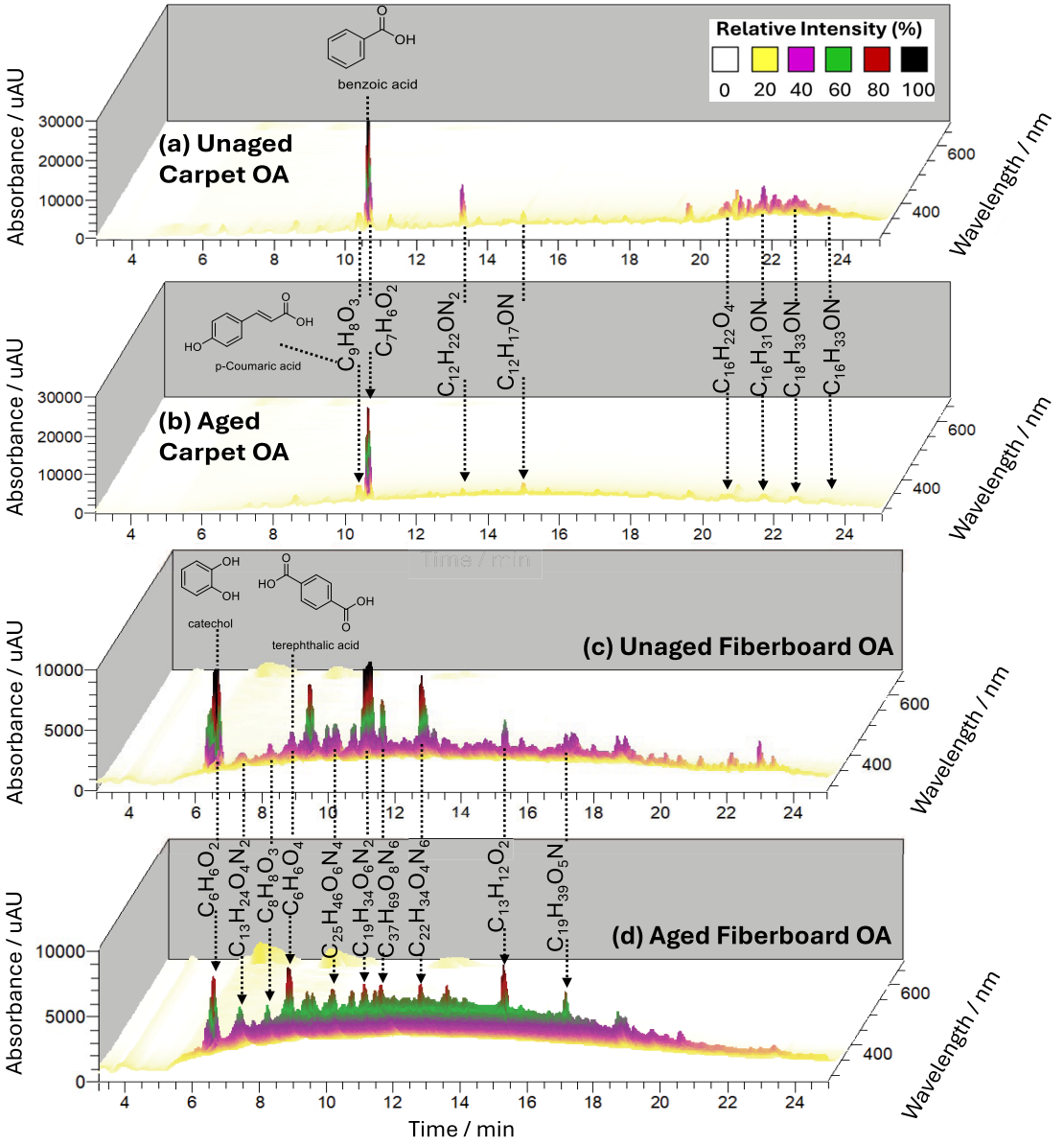

Figure 3. BrC chromophores present in the carpet and fiberboard OA samples before (a and c) and after UV aging (b and d), respectively. Benzoic acid, p-coumaric acid, catechol, and terephthalic acid were structurally identified with standards (Table S1). Note that the maximum absorbance value in the carpet and fiberboard OA panels are different. As classified in Hopstock et al.,[51] carpet OA exhibited photobleaching, whereas fiberboard OA exhibited photoenhancement after UV aging.

Figure 4 presents similar plots for vinyl flooring OA, which was previously classified as an OA type that did not exhibit a net absorbance change greater than 10% in the UV or visible wavelength ranges after photolytic aging.[51] Terephthalic acid, the main light absorbing species in unaged vinyl flooring OA, decreased in intensity by a factor of 3 after aging. However, more nonpolar and nitrogen-containing species, eluting between 17 and 25 min, increased in relative absorbance after aging. These transformations, in combination, counteracted each other, resulting in the "no change" overall optical classification. For all cases discussed, the bulk of absorption occurred at UV wavelengths, with slight increases observed in the visible wavelength regions upon aging. These observations are consistent with the absorption measurements reported in our previous work and the general definition of BrC.[30,51]

Figure 5 displays double bond equivalent (DBE) as a function of the number of (C+N) atoms calculated for assigned CH, CHO, and CHON species in the unaged (blue) and aged (red) carpet, vinyl flooring, and drywall OA. The remaining OA types can be found in Figures S5 and S6. DBE represents the total number of rings and π-bonds within an assigned species. The shaded region within the dashed reference lines illustrates the BrC-relevant space, with the upper bound representing fullerene-like hydrocarbons (DBE = 0.9 × C) and the lower bound representing linear polyenes C_xH_{x+2} (DBE = 0.5 × C).[27,37,52] Organic molecules that efficiently absorb light tend to have an uninterrupted conjugation of π-bonds across significant parts of the molecular structure.[37,53] Fullerene-like hydrocarbons exhibit the most conjugation and potential for light absorption,[54] and linear polyenes can be reasonably strong absorbers in select cases (for example, retinal has an orange color). Therefore, species with DBE/(C+N) ratios that fall within the shaded region are potentially aromatic and can act as BrC chromophores.[52,53,55]

https://doi.org/10.1021/acsestair.4c00215
ACS EST Air 2024, 1, 1495−1506

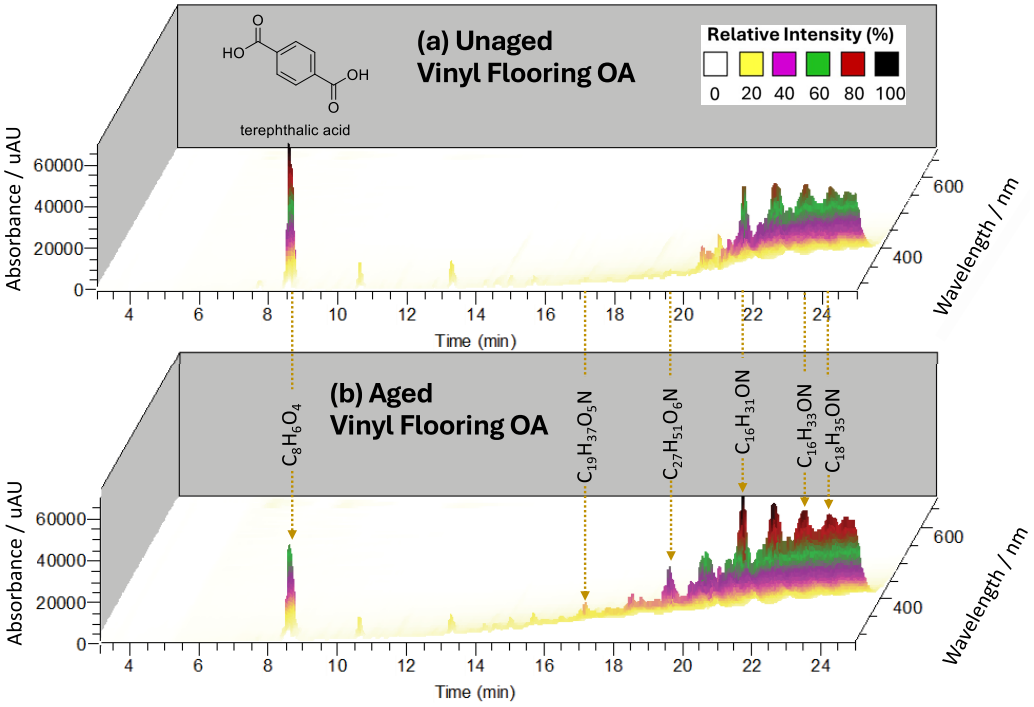

Figure 4. BrC chromophores present in the vinyl flooring OA sample before (a) and after UV aging (b). Terephthalic acid was verified with an internal standard (Table S1). As classified in Hopstock et al.,[51] vinyl flooring OA exhibited no net change in the overall absorbance after aging.

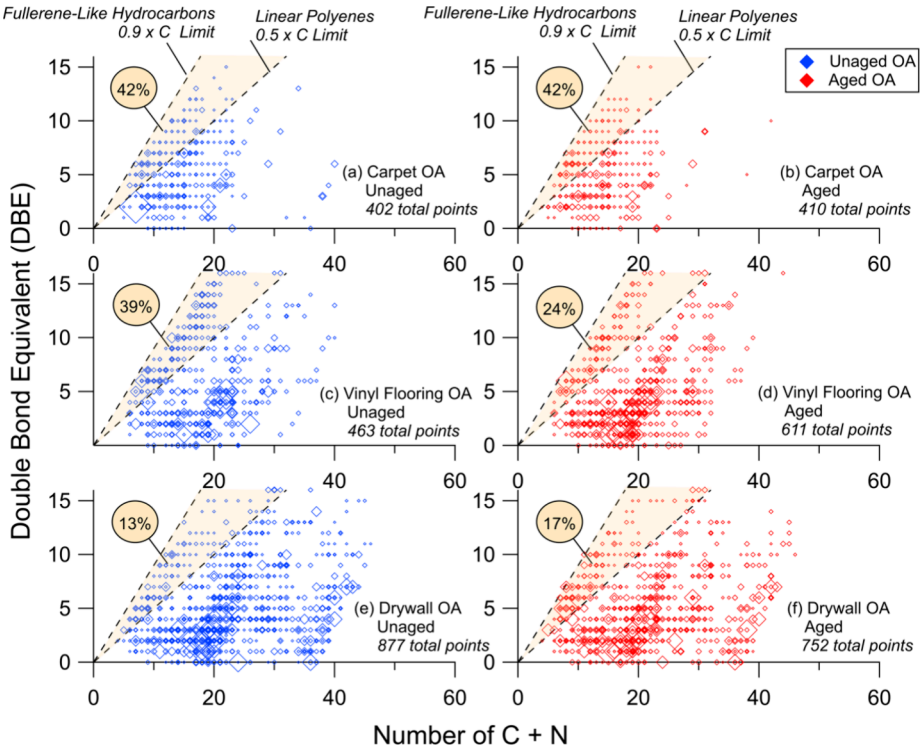

Figure 5. Plot of double bond equivalent (DBE) versus the number of carbon and nitrogen (C+N) atoms for assigned OA species in unaged and aged carpet (a and b), vinyl flooring (c and d), and drywall (e and f) OA. The size of each symbol is arbitrarily scaled to the cubic root of the corresponding MS peak intensity in order to display both stronger and weaker peaks. Reference lines indicate DBE/(C+N) values corresponding to fullerene-like hydrocarbons (0.9 × C limit) and linear polyenes (0.5 × C limit).[37,52] Yellow circles represent the percentage of data points (by number) that fall within the dashed lines and orange shaded region, thus predicted to be potential BrC chromophores. The total number of points is provided in each panel. The presented data come from both the positive and negative ionization modes. For all formulas, the number of nitrogen atoms ($N \leq 6$) is much smaller than the number of the carbon atoms.

Figures 5, S5, and S6 demonstrated the presence of BrC compounds in all ten OA types with DBE/(C+N) ratios greater than the linear polyenes limit. Across all OA samples, between 13 and 42% of all assigned compounds (by number)

https://doi.org/10.1021/acsestair.4c00215
ACS EST Air 2024, 1, 1495−1506

were potential aromatic BrC chromophores. All cases exhibited a sizable fraction of compounds beneath the linear polyenes reference line, which were not likely to be chromophoric species.

Upon photolysis, the percentage of potential chromophores remained largely unchanged (≤5% variation) for all OA except for vinyl flooring (Figure 5c,d) and fiberboard (Figure S6e,f), which exhibited reductions of 15% and 10% in the number of chromophores with aging, respectively. Although there were minor changes in the number of detected chromophores, there were more substantial changes in the relative intensities of individual BrC chromophores, which may be responsible for the previously observed photobleaching and photoenhancement behaviors. Specifically, carpet OA, a material that photobleached, displayed fewer intense peaks (smaller markers) in the aged OA (Figure 5b) compared to the unaged sample (Figure 5a). Both photobleached samples of carpet and thin PVC wire OA (Figure 5a,b and Figure S6a,b) showed a reduction in aromaticity after aging, as peak grouping and higher intensity peaks (larger markers) fell below the linear polyenes line. Aged vinyl flooring OA (Figure 5d) exhibited an overall reduction in the number of BrC chromophores, but there was a relative increase by a factor of 1.3 in the intensity of a $C_8H_6O_4$ BrC chromophore (DBE= 6, C+N = 8). Drywall OA, which photoenhanced after aging, not only had a 4% increase in the total number of BrC chromophores, but also displayed growth in individual chromophores (Figure 5e,f). Specifically, a $C_8H_8O_3$ BrC chromophore (DBE= 5, C+N= 8) increased in relative intensity by a factor of 1.5 after aging and may be the source of the photoenhancement observed in this sample. Previous literature reports that strongly absorbing BrC substituents represent a minority fraction (typically <1%) of ambient BBOA mass, and even minor changes in these minor species can have a disproportionate effect on the bulk BrC absorption.[56] The same principle applies to the OA samples studied here. In summary, although the number of detected compounds that fell within the BrC wedge remained steady, the changes in peak abundances did correlate with previous optical observations.

Structurally Identified BrC Species in OA. Structural validation of BrC chromophores in ambient samples has been a focus of many studies, as combustion mixtures possess a wide variety of compound classes and strucutres.[25,29,34,57,59,67] Jen et al. reported that over 3000 different compounds were detected in PM from wildfires, and they were successful in identifying about half of these compounds.[58] As UHPLC-PDA-HRMS analysis targeting BrC species has not been conducted for PM from the WUI, we relied upon BrC standards prepared and characterized by Moschos et al.[27] and applied them to our OA data set. A list of all 100 standard compounds can be found in Moschos et al.[27] All OA HRMS files were input into the Compound Discover program and cross-referenced with the BrC standard compounds within the internally constructed mzVault library. Each ionization mode was processed separately. Matches were determined based on retention times and MS^2 spectra. Table S1 lists the 36 BrC species present in the analyzed OA that were positively identified with the standards, and Figure S7 presents their extracted ion chromatograms (EICs), labeled with numbers corresponding to the table.[27] We will discuss a few of the structurally identified species below as they apply to the urban materials chosen for this study. It is interesting to note that many of the same organic BrC species found in BBOA were also found in the OA samples of this study.

Salicylic acid ($C_7H_6O_3$, m/z 137.0240 (−)) was the only BrC standard compound to appear in all ten OA samples. It is commonly recognized as an atmospheric tracer for biomass burning (e.g., deciduous trees and woody biomass) and, now for the first time, has been observed in PM from combusted urban materials.[59−61] Other organic acids (phthalic acid, vanillic acid, homovanillic acid, caffeic acid, terephthalic acid, p-coumaric acid, sinapinic acid, benzoic acid, and *trans*-cinnamic acid) were observed in at least three of the OA samples. PAH-like species, including 2,7-dihydroxynaphthalene, psoralen, xanthone, and 9-fluorenone were detected in various OAs through ionization in the positive mode. Plywood and lumber OA exclusively shared six confirmed BrC species (pyrogallol, 5-hydroxymethylfurfural, coniferaldehyde, 4-methylumbelliferone, 2,4-dinitrophenol, and 7-hydroxy-3,4,8-trimethylcoumarin), which are known to be biomass-derived compounds produced from the dehydration of glucose sugars (within biomass) and the thermal decomposition of lignin.[29,62−66] As plywood and lumber were the urban building materials that most resembled biomass, the crossover between literature on BBOA chromophores and those presented herein was not surprising for these two OA samples.

Phthalic acid ($C_8H_6O_4$, m/z 167.0335 (+) and 165.0189 (−)) was observed in all OA samples except drywall and fiberboard. It was the main UV chromophore in the thin PVC wire OA sample[51] and could perhaps be a potential tracer species for WUI fires. Phthalic acid may have been produced from di(2-ethylhexyl)phthalate (DEHP),[67] which is widely used as a plasticizer in PVC plastics,[68] building and furniture materials (including furniture upholstery, mattresses, wall coverings, floor tiles, and vinyl flooring),[69] and many other consumer products.[70] The presence of phthalic acid in eight out of ten OA samples tested may indicate the presence of DEHP plasticizers in uncombusted urban materials. Carpet OA exhibited phthalic acid most likely due to the PVC vinyl backing applied to the bottom of the carpet pile fibers. Another example of a plastic precursor, terephthalic acid, was found in vinyl flooring, plywood, and fiberboard OA. Terephthalic acid is a key precursor to polyethylene terephthalate (PET), which is commonly used in the manufacture of products that require a barrier to gases (CO_2 and O_2) and resistance to shattering.[71] As is the case for all species highlighted in this study, we cannot ignore other atmospheric emission sources can be responsible for their prevalence in ambient samples. For instance, phthalic acid is a well-known product from naphthalene photooxidation and is often used as a tracer of naphthalene-derived secondary organic aerosol.[72]

NACs are known to be major contributors to light absorption in biomass burning BrC.[42] The BrC standard mixture contained 11 NAC species commonly found in BBOA,[27] and of these, only two species (4-nitrophenol and 2,4-dinitrophenol) were present in OA samples. 4-Nitrophenol ($C_6H_5NO_3$, m/z 138.0193 (−)) was detected in all OA samples except carpet, thick PVC wire, and fiberboard, whereas 2,4-dinitrophenol ($C_6H_4N_2O_5$, m/z 183.0043 (−)) was only present in plywood, fiberboard, and lumber OA. The absence of other NACs in urban material OA could indicate that the nondetected NACs (e.g., 4-nitrocatechol, 5-nitrosalicylic acid, 2-nitrophenol, and 4-nitro-o-cresol) are more indicative of traditional biomass fires. As this study only surveyed ten urban materials and was carried out in the absence of oxygen during

https://doi.org/10.1021/acsestair.4c00215
ACS EST Air 2024, 1, 1495−1506

pyrolysis, additional testing of more urban material OA types is needed to determine if this trend holds.

Tentatively Assigned Species Unique to Each OA. Table S2 presents tentatively assigned species that were among the highest intensity peaks and unique to each urban material. We will briefly summarize our findings here but note that these assignments have not been confirmed with standards, and only the observed m/z values are reliable. Details on the usages of each species were found in previous literature and the PubChem database (National Library of Medicine).

Carpet OA's selected unique species were nitrogen-containing (e.g., 4-hydroxyquinazoline ($C_8H_6N_2O$) and 2-methyl-1,4-piperazine dicarbaldehyde ($C_7H_{12}N_2O_2$)). We were unable to find species which were both unique to carpet OA and clearly associated with urban additives and/or manufacturing. Thin PVC wire OA uniquely contained 1,2,4-benzenetricarboxylic acid ($C_9H_6O_6$, an intermediate for resins, plasticizers, dyes, inks, and adhesives), 2-(2-aminobenzoyl) benzoic acid ($C_{14}H_{11}NO_3$, a dye intermediate), and benzanilide ($C_{13}H_{11}NO$, used in dye making).[73,74] Vinyl flooring OA was distinguished from all other materials by its large PAH structures. These species (xanthone ($C_{13}H_8O_2$) and 9-fluorenone ($C_{13}H_8O$) from Table S1 (structurally identified), and 5,6a-dihydronaphtho[2,1,8,7-klmn]xanthene ($C_{18}H_{10}O$), naphthanthrone ($C_{19}H_{10}O$), 7-hydroxymethyl-12-methylbenz[a]anthracene ($C_{20}H_{16}O$), and benzo[k]-tetraphene-5-ol ($C_{22}H_{14}O$) from Table S2 (tentatively assigned)), were resistant to UV induced change, as they were present in both the unaged and aged OA, and their abundances may have contributed to the optical classification of "no change". Fabric OA presented with the unique species dihexyl phthalate ($C_{20}H_{30}O_4$), often used in textiles and vinyl upholstery (as was the case for this fabric material).[73] Plywood OA's unique markers included resorcinol ($C_6H_6O_2$, used in plastic production),[75] reticulol ($C_{11}H_{10}O_5$), 2-(2-hydroxyethoxycarbonyl) benzoic acid ($C_{10}H_{10}O_5$, patented for resins used in forming multilayer coating films and adhesives),[76] 10-undecenoic acid ($C_{11}H_{20}O_2$, used as a precursor in the manufacture of polymers),[77] and others listed in Table S2. Given that plywood is made up of sheets of wood that are adhered together, it is likely that the species found here were utilized in the manufacturing processes of this plywood material. Ceiling tile OA presented with bis(2-ethylhexyl) amine ($C_{16}H_{35}N$), which is patented as a modified epoxy resin and may have been used to adhere components together.[78] Thick PVC wire OA exhibited 1-(4-hydroxyphenyl)-2-phenylethan-1-one ($C_{14}H_{12}O_2$, patented as a resin)[79] and laurixamine ($C_{15}H_{33}NO$, used in production of polymers and metallic pigments).[80] Note that both thin and thick PVC wire OA have unique species that are predicted to be resins, plasticizers, and ink/dye species. These two coated wires were different in manufacturer, color, and thickness of PVC coating, illustrating the wide variety of species that can be emitted even from one class of urban material. Drywall OA did not possess many unique species that had structural matches to online databases referenced by the Compound Discover program. We observed large ions corresponding to $C_{19}H_{35}NO_5$ and $C_{19}H_{38}N_2O$. Drywall is composed of calcium sulfate dihydrate (gypsum) with additives of plasticizers, foaming agents, cellulose, and fiberglass. Preliminary results from Compound Discover showed many sulfur-containing species for this OA type only. Due to CHON assignment restraints implemented in this pilot study, we did not report sulfur-containing organics in this work, but future studies from our group will incorporate a greater heteroatom variety in the analysis. Fiberboard OA exhibited 3-methyl-2-quinoxalinecarboxylic acid ($C_{10}H_8N_2O_2$, an eye irritant)[73] and 3-hydroxy-2-napthohydrazide ($C_{11}H_{10}N_2O_2$, an epoxy resin for fiber reinforced composite materials).[81] Lumber OA exhibited unique markers potentially assigned to methylsuccinic acid ($C_5H_8O_4$) and acetic propanoic anhydride ($C_5H_8O_3$).

ATMOSPHERIC IMPLICATIONS

This work serves as a pilot study for the chemical characterization of OA produced in WUI fires, and the effect of photolytic aging on this OA. One of the key findings is that photolytic aging results in relatively small changes to the overall chemical composition despite having a large impact on the overall absorption coefficient of OA (i.e., photobleaching and photoenhancement effects). This reinforces previous observations that the optical absorption of BrC is controlled by a small fraction of chromophoric species. Changes in the relative intensity of these species are difficult to notice because they are obscured by more abundant nonabsorbing species.

It is important to note that this study only focused on a small variety of species present in WUI fires. Additionally, OA was generated only at a single pyrolysis temperature (600 °C), and in the absence of oxygen. This is not fully representative of environmental fires, which often oscillate between smoldering and flaming combustion, with flaming temperatures reaching at least an order of magnitude higher than smoldering or pyrolysis. Results in this work are also limited in that we only focused on CHON species when characterizing BrC species. Metals and halogenated species are expected to be produced through the combustion of human made materials. Future studies should burn a greater variety of urban materials (such as those containing perfluoroalkyl and polyfluoroalkyl substances) under more diverse combustion conditions and determine the molecular composition and long-term photochemical transformations of largescale WUI fires. Here, we have provided tentatively assigned species for each OA type (Table S2) and, in the future, these species can be structurally identified to build a library of compounds signature to WUI fires.

ASSOCIATED CONTENT

Supporting Information

The Supporting Information is available free of charge at https://pubs.acs.org/doi/10.1021/acsestair.4c00215.

Procedure for generating and collecting pyrolysis samples, additional description of UHPLC−PDA−HRMS sample preparation and analysis, TIC chromatograms for all the samples, principal component analysis of the observed compounds in samples, PDA chromatograms before and after photolysis for select samples, graphs of DBE as a function of the number of (C+N) atoms for all samples, a table of positively identified species, and a table of unique species in different samples (PDF)

AUTHOR INFORMATION

Corresponding Author

Sergey A. Nizkorodov − *Department of Chemistry, University of California, Irvine, Irvine, California 92697, United States;*

https://doi.org/10.1021/acsestair.4c00215
ACS EST Air 2024, 1, 1495−1506

orcid.org/0000-0003-0891-0052; Email: nizkorod@uci.edu

Authors

Katherine S. Hopstock − *Department of Chemistry, University of California, Irvine, Irvine, California 92697, United States;* orcid.org/0000-0001-9141-8899

Qiaorong Xie − *Department of Chemistry, Purdue University, West Lafayette, Indiana 47907, United States;* orcid.org/0000-0002-9391-624X

Michael A. Alvarado − *Department of Chemistry, University of California, Irvine, Irvine, California 92697, United States*

Vaios Moschos − *Department of Physics, North Carolina Agricultural and Technical State University, Greensboro, North Carolina 27411, United States; Department of Environmental Sciences and Engineering, Gillings School of Global Public Health, The University of North Carolina at Chapel Hill, Chapel Hill, North Carolina 27599, United States;* orcid.org/0000-0002-6251-4117

Solomon Bililign − *Department of Physics, North Carolina Agricultural and Technical State University, Greensboro, North Carolina 27411, United States*

Jason D. Surratt − *Department of Environmental Sciences and Engineering, Gillings School of Global Public Health, The University of North Carolina at Chapel Hill, Chapel Hill, North Carolina 27599, United States; Department of Chemistry, College Arts and Sciences, The University of North Carolina at Chapel Hill, Chapel Hill, North Carolina 27599, United States;* orcid.org/0000-0002-6833-1450

Alexander Laskin − *Department of Chemistry, Purdue University, West Lafayette, Indiana 47907, United States; Department of Earth, Atmospheric and Planetary Sciences, West Lafayette, Indiana 47907, United States;* orcid.org/0000-0002-7836-8417

Complete contact information is available at: https://pubs.acs.org/10.1021/acsestair.4c00215

Notes

The authors declare no competing financial interest.

■ ACKNOWLEDGMENTS

This study was supported by the National Oceanic and Atmospheric Administration grants NA22OAR4310196 (University of California, Irvine) and NA22OAR4310195 (Purdue University). Reference standards used in this study were made possible by a US National Science Foundation (NSF) grant # 2100708 (NCA&T University), which was through the Atmospheric and Geospace Sciences (AGS) Division. V.M. acknowledges support in part by the Swiss National Science Foundation (SNSF) under the Postdoc Mobility Fellowship grant P500PN_210745. The authors thank Diego Calderon-Arrieta (Purdue University) for assistance in learning MZmine data processing and Dr. Veronique Perraud and Adam Thomas (University of California, Irvine) for assistance with MzVault and Compound Discover programs.

■ REFERENCES

(1) National Academies of Sciences, Engineering, and Medicine. *The Chemistry of Fires at the Wildland-Urban Interface*; National Academies Press (US): Washington, D.C., 2022. DOI: 10.17226/26460.

(2) Shuman, J. K.; Balch, J. K.; Barnes, R. T.; Higuera, P. E.; Roos, C. I.; Schwilk, D. W.; Stavros, E. N.; Banerjee, T.; Bela, M. M.; Bendix, J.; Bertolino, S.; Bililign, S.; Bladon, K. D.; Brando, P.; Breidenthal, R. E.; Buma, B.; Calhoun, D.; Carvalho, L. M. V.; Cattau, M. E.; Cawley, K. M.; Chandra, S.; Chipman, M. L.; Cobian-Iñiguez, J.; Conlisk, E.; Coop, J. D.; Cullen, A.; Davis, K. T.; Dayalu, A.; De Sales, F.; Dolman, M.; Ellsworth, L. M.; Franklin, S.; Guiterman, C. H.; Hamilton, M.; Hanan, E. J.; Hansen, W. D.; Hantson, S.; Harvey, B. J.; Holz, A.; Huang, T.; Hurteau, M. D.; Ilangakoon, N. T.; Jennings, M.; Jones, C.; Klimaszewski-Patterson, A.; Kobziar, L. N.; Kominoski, J.; Kosovic, B.; Krawchuk, M. A.; Laris, P.; Leonard, J.; Loria-Salazar, S. M.; Lucash, M.; Mahmoud, H.; Margolis, E.; Maxwell, T.; McCarty, J. L.; McWethy, D. B.; Meyer, R. S.; Miesel, J. R.; Moser, W. K.; Nagy, R. C.; Niyogi, D.; Palmer, H. M.; Pellegrini, A.; Poulter, B.; Robertson, K.; Rocha, A. V.; Sadegh, M.; Santos, F.; Scordo, F.; Sexton, J. O.; Sharma, A. S.; Smith, A. M. S.; Soja, A. J.; Still, C.; Swetnam, T.; Syphard, A. D.; Tingley, M. W.; Tohidi, A.; Trugman, A. T.; Turetsky, M.; Varner, J. M.; Wang, Y.; Whitman, T.; Yelenik, S.; Zhang, X. Reimagine Fire Science for the Anthropocene. *PNAS Nexus* **2022**, *1* (3), No. pgac115.

(3) Radeloff, V. C.; Helmers, D. P.; Kramer, H. A.; Mockrin, M. H.; Alexandre, P. M.; Bar-Massada, A.; Butsic, V.; Hawbaker, T. J.; Martinuzzi, S.; Syphard, A. D.; Stewart, S. I. Rapid Growth of the US Wildland-Urban Interface Raises Wildfire Risk. *Proc. Natl. Acad. Sci. U. S. A.* **2018**, *115* (13), 3314−3319.

(4) Calkin, D. E.; Cohen, J. D.; Finney, M. A.; Thompson, M. P. How Risk Management Can Prevent Future Wildfire Disasters in the Wildland-Urban Interface. *Proc. Natl. Acad. Sci. U. S. A.* **2014**, *111* (2), 746−751.

(5) Burke, M.; Driscoll, A.; Heft-Neal, S.; Xue, J.; Burney, J.; Wara, M. The Changing Risk and Burden of Wildfire in the United States. *Proc. Natl. Acad. Sci. U. S. A.* **2021**, *118* (2), No. e2011048118.

(6) Fernandez-Pello, A. C. Wildland Fire Spot Ignition by Sparks and Firebrands. *Fire Safety Journal* **2017**, *91*, 2−10.

(7) Manzello, S. L.; Suzuki, S.; Hayashi, Y. Enabling the Study of Structure Vulnerabilities to Ignition from Wind Driven Firebrand Showers: A Summary of Experimental Results. *Fire Safety Journal* **2012**, *54*, 181−196.

(8) Manzello, S. L.; Quarles, S. L. Special Section on Structure Ignition in Wildland-Urban Interface (WUI) Fires. *Fire Technol.* **2017**, *53* (2), 425−427.

(9) Santoso, M. A.; Christensen, E. G.; Yang, J.; Rein, G. Review of the Transition From Smouldering to Flaming Combustion in Wildfires. *Front. Mech. Eng.* **2019**, *5*, 49.

(10) Robinson, A. L.; Donahue, N. M.; Shrivastava, M. K.; Weitkamp, E. A.; Sage, A. M.; Grieshop, A. P.; Lane, T. E.; Pierce, J. R.; Pandis, S. N. Rethinking Organic Aerosols: Semivolatile Emissions and Photochemical Aging. *Science* **2007**, *315* (5816), 1259−1262.

(11) Akherati, A.; Cappa, C. D.; Kleeman, M. J.; Docherty, K. S.; Jimenez, J. L.; Griffith, S. M.; Dusanter, S.; Stevens, P. S.; Jathar, S. H. Simulating Secondary Organic Aerosol in a Regional Air Quality Model Using the Statistical Oxidation Model − Part 3: Assessing the Influence of Semi-Volatile and Intermediate-Volatility Organic Compounds and NO_x. *Atmospheric Chemistry and Physics* **2019**, *19* (7), 4561−4594.

(12) Stec, A. A.; Hull, T. R. Assessment of the Fire Toxicity of Building Insulation Materials. *Energy and Buildings* **2011**, *43* (2), 498−506.

(13) Stec, A. A.; Readman, J.; Blomqvist, P.; Gylestam, D.; Karlsson, D.; Wojtalewicz, D.; Dlugogorski, B. Z. Analysis of Toxic Effluents Released from PVC Carpet under Different Fire Conditions. *Chemosphere* **2013**, *90* (1), 65−71.

(14) Blomqvist, P.; McNamee, M. S.; Stec, A. A.; Gylestam, D.; Karlsson, D. Detailed Study of Distribution Patterns of Polycyclic Aromatic Hydrocarbons and Isocyanates under Different Fire Conditions. *Fire and Materials* **2014**, *38* (1), 125−144.

(15) Samburova, V.; Connolly, J.; Gyawali, M.; Yatavelli, R. L. N.; Watts, A. C.; Chakrabarty, R. K.; Zielinska, B.; Moosmüller, H.; Khlystov, A. Polycyclic Aromatic Hydrocarbons in Biomass-Burning Emissions and Their Contribution to Light Absorption and Aerosol Toxicity. *Science of The Total Environment* **2016**, *568*, 391−401.

(16) Lin, P.; Aiona, P. K.; Li, Y.; Shiraiwa, M.; Laskin, J.; Nizkorodov, S. A.; Laskin, A. Molecular Characterization of Brown Carbon in Biomass Burning Aerosol Particles. *Environ. Sci. Technol.* **2016**, *50* (21), 11815−11824.
(17) Blomqvist, P.; Rosell, L.; Simonson, M. Emissions from Fires Part II: Simulated Room Fires. *Fire Technol.* **2004**, *40* (1), 59−73.
(18) Hedman, B.; Näslund, M.; Nilsson, C.; Marklund, S. Emissions of Polychlorinated Dibenzodioxins and Dibenzofurans and Polychlorinated Biphenyls from Uncontrolled Burning of Garden and Domestic Waste (Backyard Burning). *Environ. Sci. Technol.* **2005**, *39* (22), 8790−8796.
(19) Chong, N. S.; Abdulramoni, S.; Patterson, D.; Brown, H. Releases of Fire-Derived Contaminants from Polymer Pipes Made of Polyvinyl Chloride. *Toxics* **2019**, *7* (4), 57.
(20) Laing, J. R.; Jaffe, D. A.; Hee, J. R. Physical and Optical Properties of Aged Biomass Burning Aerosol from Wildfires in Siberia and the Western USA at the Mt. Bachelor Observatory. *Atmospheric Chemistry and Physics* **2016**, *16* (23), 15185−15197.
(21) Zhou, S.; Collier, S.; Jaffe, D. A.; Briggs, N. L.; Hee, J.; Sedlacek III, A. J.; Kleinman, L.; Onasch, T. B.; Zhang, Q. Regional Influence of Wildfires on Aerosol Chemistry in the Western US and Insights into Atmospheric Aging of Biomass Burning Organic Aerosol. *Atmospheric Chemistry and Physics* **2017**, *17* (3), 2477−2493.
(22) Konovalov, I. B.; Beekmann, M.; Berezin, E. V.; Petetin, H.; Mielonen, T.; Kuznetsova, I. N.; Andreae, M. O. The Role of Semi-Volatile Organic Compounds in the Mesoscale Evolution of Biomass Burning Aerosol: A Modeling Case Study of the 2010 Mega-Fire Event in Russia. *Atmospheric Chemistry and Physics* **2015**, *15* (23), 13269−13297.
(23) Capes, G.; Johnson, B.; McFiggans, G.; Williams, P. I.; Haywood, J.; Coe, H. Aging of Biomass Burning Aerosols over West Africa: Aircraft Measurements of Chemical Composition, Microphysical Properties, and Emission Ratios. *Journal of Geophysical Research: Atmospheres* **2008**, *113* (D23), No. D00C15.
(24) Smith, D. M.; Fiddler, M. N.; Pokhrel, R. P.; Bililign, S. Laboratory Studies of Fresh and Aged Biomass Burning Aerosol Emitted from East African Biomass Fuels − Part 1: Optical Properties. *Atmospheric Chemistry and Physics* **2020**, *20* (17), 10149−10168.
(25) Smith, D. M.; Cui, T.; Fiddler, M. N.; Pokhrel, R. P.; Surratt, J. D.; Bililign, S. Laboratory Studies of Fresh and Aged Biomass Burning Aerosol Emitted from East African Biomass Fuels − Part 2: Chemical Properties and Characterization. *Atmos. Chem. Phys.* **2020**, *20* (17), 10169−10191.
(26) Bougiatioti, A.; Stavroulas, I.; Kostenidou, E.; Zarmpas, P.; Theodosi, C.; Kouvarakis, G.; Canonaco, F.; Prévôt, A. S. H.; Nenes, A.; Pandis, S. N.; Mihalopoulos, N. Processing of Biomass-Burning Aerosol in the Eastern Mediterranean during Summertime. *Atmospheric Chemistry and Physics* **2014**, *14* (9), 4793−4807.
(27) Moschos, V.; Christensen, C.; Mouton, M.; Fiddler, M. N.; Isolabella, T.; Mazzei, F.; Massabò, D.; Turpin, B. J.; Bililign, S.; Surratt, J. D. Quantifying the Light-Absorption Properties and Molecular Composition of Brown Carbon Aerosol from Sub-Saharan African Biomass Combustion. *Environ. Sci. Technol.* **2024**, *58* (9), 4268−4280.
(28) Wang, X.; Firouzkouhi, H.; Chow, J. C.; Watson, J. G.; Ho, S. S. H.; Carter, W.; De Vos, A. S. M. Chemically Speciated Air Pollutant Emissions from Open Burning of Household Solid Waste from South Africa. *Atmospheric Chemistry and Physics* **2023**, *23* (24), 15375−15393.
(29) Sekimoto, K.; Koss, A. R.; Gilman, J. B.; Selimovic, V.; Coggon, M. M.; Zarzana, K. J.; Yuan, B.; Lerner, B. M.; Brown, S. S.; Warneke, C.; Yokelson, R. J.; Roberts, J. M.; de Gouw, J. High- and Low-Temperature Pyrolysis Profiles Describe Volatile Organic Compound Emissions from Western US Wildfire Fuels. *Atmos. Chem. Phys.* **2018**, *18* (13), 9263−9281.
(30) Laskin, A.; Laskin, J.; Nizkorodov, S. A. Chemistry of Atmospheric Brown Carbon. *Chem. Rev.* **2015**, *115* (10), 4335−4382.
(31) Hopstock, K. S.; Carpenter, B. P.; Patterson, J. P.; Al-Abadleh, H. A.; Nizkorodov, S. A. Formation of Insoluble Brown Carbon through Iron-Catalyzed Reaction of Biomass Burning Organics. *Environ. Sci.: Atmos.* **2023**, *3* (1), 207−220.
(32) Huang, R.-J.; Yang, L.; Shen, J.; Yuan, W.; Gong, Y.; Ni, H.; Duan, J.; Yan, J.; Huang, H.; You, Q.; Li, Y. J. Chromophoric Fingerprinting of Brown Carbon from Residential Biomass Burning. *Environ. Sci. Technol. Lett.* **2022**, *9* (2), 102−111.
(33) Sun, H.; Biedermann, L.; Bond, T. C. Color of Brown Carbon: A Model for Ultraviolet and Visible Light Absorption by Organic Carbon Aerosol. *Geophys. Res. Lett.* **2007**, *34* (17), No. L17813.
(34) Dalton, A. B.; Nizkorodov, S. A. Photochemical Degradation of 4-Nitrocatechol and 2,4-Dinitrophenol in a Sugar-Glass Secondary Organic Aerosol Surrogate. *Environ. Sci. Technol.* **2021**, *55* (21), 14586−14594.
(35) Fleming, L. T.; Lin, P.; Roberts, J. M.; Selimovic, V.; Yokelson, R.; Laskin, J.; Laskin, A.; Nizkorodov, S. A. Molecular Composition and Photochemical Lifetimes of Brown Carbon Chromophores in Biomass Burning Organic Aerosol. *Atmospheric Chemistry and Physics* **2020**, *20* (2), 1105−1129.
(36) Lin, P.; Bluvshtein, N.; Rudich, Y.; Nizkorodov, S. A.; Laskin, J.; Laskin, A. Molecular Chemistry of Atmospheric Brown Carbon Inferred from a Nationwide Biomass Burning Event. *Environ. Sci. Technol.* **2017**, *51* (20), 11561−11570.
(37) Lin, P.; Fleming, L. T.; Nizkorodov, S. A.; Laskin, J.; Laskin, A. Comprehensive Molecular Characterization of Atmospheric Brown Carbon by High Resolution Mass Spectrometry with Electrospray and Atmospheric Pressure Photoionization. *Anal. Chem.* **2018**, *90* (21), 12493−12502.
(38) Bluvshtein, N.; Lin, P.; Flores, J. M.; Segev, L.; Mazar, Y.; Tas, E.; Snider, G.; Weagle, C.; Brown, S. S.; Laskin, A.; Rudich, Y. Broadband Optical Properties of Biomass-Burning Aerosol and Identification of Brown Carbon Chromophores. *Journal of Geophysical Research: Atmospheres* **2017**, *122* (10), 5441−5456.
(39) Claeys, M.; Vermeylen, R.; Yasmeen, F.; Gómez-González, Y.; Chi, X.; Maenhaut, W.; Mészáros, T.; Salma, I. Chemical Characterisation of Humic-like Substances from Urban, Rural and Tropical Biomass Burning Environments Using Liquid Chromatography with UV/Vis Photodiode Array Detection and Electrospray Ionisation Mass Spectrometry. *Environ. Chem.* **2012**, *9* (3), 273−284.
(40) Wang, Y.; Hu, M.; Lin, P.; Guo, Q.; Wu, Z.; Li, M.; Zeng, L.; Song, Y.; Zeng, L.; Wu, Y.; Guo, S.; Huang, X.; He, L. Molecular Characterization of Nitrogen-Containing Organic Compounds in Humic-like Substances Emitted from Straw Residue Burning. *Environ. Sci. Technol.* **2017**, *51* (11), 5951−5961.
(41) Mohr, C.; Lopez-Hilfiker, F. D.; Zotter, P.; Prévôt, A. S. H.; Xu, L.; Ng, N. L.; Herndon, S. C.; Williams, L. R.; Franklin, J. P.; Zahniser, M. S.; Worsnop, D. R.; Knighton, W. B.; Aiken, A. C.; Gorkowski, K. J.; Dubey, M. K.; Allan, J. D.; Thornton, J. A. Contribution of Nitrated Phenols to Wood Burning Brown Carbon Light Absorption in Detling, United Kingdom during Winter Time. *Environ. Sci. Technol.* **2013**, *47* (12), 6316−6324.
(42) Xie, M.; Chen, X.; Hays, M. D.; Holder, A. L. Composition and Light Absorption of N-Containing Aromatic Compounds in Organic Aerosols from Laboratory Biomass Burning. *Atmospheric Chemistry and Physics* **2019**, *19* (5), 2899−2915.
(43) Forrister, H.; Liu, J.; Scheuer, E.; Dibb, J.; Ziemba, L.; Thornhill, K. L.; Anderson, B.; Diskin, G.; Perring, A. E.; Schwarz, J. P.; Campuzano-Jost, P.; Day, D. A.; Palm, B. B.; Jimenez, J. L.; Nenes, A.; Weber, R. J. Evolution of Brown Carbon in Wildfire Plumes. *Geophys. Res. Lett.* **2015**, *42* (11), 4623−4630.
(44) Hinks, M. L.; Brady, M. V.; Lignell, H.; Song, M.; Grayson, J. W.; Bertram, A. K.; Lin, P.; Laskin, A.; Laskin, J.; Nizkorodov, S. A. Effect of Viscosity on Photodegradation Rates in Complex Secondary Organic Aerosol Materials. *Phys. Chem. Chem. Phys.* **2016**, *18* (13), 8785−8793.
(45) Selimovic, V.; Yokelson, R. J.; McMeeking, G. R.; Coefield, S. In Situ Measurements of Trace Gases, PM, and Aerosol Optical Properties during the 2017 NW US Wildfire Smoke Event. *Atmospheric Chemistry and Physics* **2019**, *19* (6), 3905−3926.

https://doi.org/10.1021/acsestair.4c00215
ACS EST Air 2024, 1, 1495−1506

(46) Saleh, R. From Measurements to Models: Toward Accurate Representation of Brown Carbon in Climate Calculations. *Curr. Pollution Rep* **2020**, *6* (2), 90−104.
(47) Laskin, J.; Laskin, A.; Nizkorodov, S. A. Mass Spectrometry Analysis in Atmospheric Chemistry. *Anal. Chem.* **2018**, *90* (1), 166−189.
(48) Moise, T.; Flores, J. M.; Rudich, Y. Optical Properties of Secondary Organic Aerosols and Their Changes by Chemical Processes. *Chem. Rev.* **2015**, *115* (10), 4400−4439.
(49) Di Lorenzo, R. A.; Washenfelder, R. A.; Attwood, A. R.; Guo, H.; Xu, L.; Ng, N. L.; Weber, R. J.; Baumann, K.; Edgerton, E.; Young, C. J. Molecular-Size-Separated Brown Carbon Absorption for Biomass-Burning Aerosol at Multiple Field Sites. *Environ. Sci. Technol.* **2017**, *51* (6), 3128−3137.
(50) Calderon-Arrieta, D.; Morales, A. C.; Hettiyadura, A. P. S.; Estock, T. M.; Li, C.; Rudich, Y.; Laskin, A. Enhanced Light Absorption and Elevated Viscosity of Atmospheric Brown Carbon through Evaporation of Volatile Components. *Environ. Sci. Technol.* **2024**, *58* (17), 7493−7504.
(51) Hopstock, K. S.; Klodt, A. L.; Xie, Q.; Alvarado, M. A.; Laskin, A.; Nizkorodov, S. A. Photolytic Aging of Organic Aerosol from Pyrolyzed Urban Materials. *Environ. Sci.: Atmos.* **2023**, *3* (9), 1272−1285.
(52) Siemens, K.; Morales, A.; He, Q.; Li, C.; Hettiyadura, A. P. S.; Rudich, Y.; Laskin, A. Molecular Analysis of Secondary Brown Carbon Produced from the Photooxidation of Naphthalene. *Environ. Sci. Technol.* **2022**, *56* (6), 3340−3353.
(53) West, C. P.; Hettiyadura, A. P. S.; Darmody, A.; Mahamuni, G.; Davis, J.; Novosselov, I.; Laskin, A. Molecular Composition and the Optical Properties of Brown Carbon Generated by the Ethane Flame. *ACS Earth Space Chem.* **2020**, *4* (7), 1090−1103.
(54) Lobodin, V. V.; Marshall, A. G.; Hsu, C. S. Compositional Space Boundaries for Organic Compounds. *Anal. Chem.* **2012**, *84* (7), 3410−3416.
(55) Siemens, K. S. A.; Pagonis, D.; Guo, H.; Schueneman, M. K.; Dibb, J. E.; Campuzano-Jost, P.; Jimenez, J. L.; Laskin, A. Probing Atmospheric Aerosols by Multimodal Mass Spectrometry Techniques: Revealing Aging Characteristics of Its Individual Molecular Components. *ACS Earth Space Chem.* **2023**, *7* (12), 2498−2510.
(56) Budisulistiorini, S. H.; Riva, M.; Williams, M.; Chen, J.; Itoh, M.; Surratt, J. D.; Kuwata, M. Light-Absorbing Brown Carbon Aerosol Constituents from Combustion of Indonesian Peat and Biomass. *Environ. Sci. Technol.* **2017**, *51* (8), 4415−4423.
(57) Nozière, B.; Kalberer, M.; Claeys, M.; Allan, J.; D'Anna, B.; Decesari, S.; Finessi, E.; Glasius, M.; Grgić, I.; Hamilton, J. F.; Hoffmann, T.; Iinuma, Y.; Jaoui, M.; Kahnt, A.; Kampf, C. J.; Kourtchev, I.; Maenhaut, W.; Marsden, N.; Saarikoski, S.; Schnelle-Kreis, J.; Surratt, J. D.; Szidat, S.; Szmigielski, R.; Wisthaler, A. The Molecular Identification of Organic Compounds in the Atmosphere: State of the Art and Challenges. *Chem. Rev.* **2015**, *115* (10), 3919−3983.
(58) Jen, C. N.; Hatch, L. E.; Selimovic, V.; Yokelson, R. J.; Weber, R.; Fernandez, A. E.; Kreisberg, N. M.; Barsanti, K. C.; Goldstein, A. H. Speciated and Total Emission Factors of Particulate Organics from Burning Western US Wildland Fuels and Their Dependence on Combustion Efficiency. *Atmos. Chem. Phys.* **2019**, *19* (2), 1013−1026.
(59) Hoffer, A.; Tóth, Á.; Jancsek-Turóczi, B.; Machon, A.; Meiramova, A.; Nagy, A.; Marmureanu, L.; Gelencsér, A. Potential New Tracers and Their Mass Fraction in the Emitted PM_{10} from the Burning of Household Waste in Stoves. *Atmospheric Chemistry and Physics* **2021**, *21* (23), 17855−17864.
(60) Sengupta, D.; Samburova, V.; Bhattarai, C.; Watts, A. C.; Moosmüller, H.; Khlystov, A. Y. Polar Semivolatile Organic Compounds in Biomass-Burning Emissions and Their Chemical Transformations during Aging in an Oxidation Flow Reactor. *Atmospheric Chemistry and Physics* **2020**, *20* (13), 8227−8250.
(61) Li, W.; Ge, P.; Chen, M.; Tang, J.; Cao, M.; Cui, Y.; Hu, K.; Nie, D. Tracers from Biomass Burning Emissions and Identification of Biomass Burning. *Atmosphere* **2021**, *12* (11), 1401.
(62) Liang, Y.; Jen, C. N.; Weber, R. J.; Misztal, P. K.; Goldstein, A. H. Chemical Composition of PM2.5 in October 2017 Northern California Wildfire Plumes. *Atmos. Chem. Phys.* **2021**, *21* (7), 5719−5737.
(63) Liu-Kang, C.; Gallimore, P. J.; Liu, T.; Abbatt, J. P. D. Photoreaction of Biomass Burning Brown Carbon Aerosol Particles. *Environmental Science: Atmospheres* **2022**, *2* (2), 270−278.
(64) Yuan, W.; Huang, R.-J.; Yang, L.; Guo, J.; Chen, Z.; Duan, J.; Wang, T.; Ni, H.; Han, Y.; Li, Y.; Chen, Q.; Chen, Y.; Hoffmann, T.; O'Dowd, C. Characterization of the Light-Absorbing Properties, Chromophore Composition and Sources of Brown Carbon Aerosol in Xi'an, Northwestern China. *Atmos. Chem. Phys.* **2020**, *20* (8), 5129−5144.
(65) Jiang, F.; Song, J.; Bauer, J.; Gao, L.; Vallon, M.; Gebhardt, R.; Leisner, T.; Norra, S.; Saathoff, H. Chromophores and Chemical Composition of Brown Carbon Characterized at an Urban Kerbside by Excitation−Emission Spectroscopy and Mass Spectrometry. *Atmospheric Chemistry and Physics* **2022**, *22* (22), 14971−14986.
(66) Menegazzo, F.; Ghedini, E.; Signoretto, M. 5-Hydroxymethylfurfural (HMF) Production from Real Biomasses. *Molecules* **2018**, *23* (9), 2201.
(67) Mettang, T.; Alscher, D. M.; Pauli-Magnus, C.; Dunst, R.; Kuhlmann, U.; Rettenmeier, A. W. Phthalic Acid Is the Main Metabolite of the Plasticizer Di(2-Ethylhexyl) Phthalate in Peritoneal Dialysis Patients. *Adv. Perit Dial* **1999**, *15*, 229−233.
(68) Earls, A. O.; Axford, I. P.; Braybrook, J. H. Gas Chromatography−Mass Spectrometry Determination of the Migration of Phthalate Plasticisers from Polyvinyl Chloride Toys and Childcare Articles. *Journal of Chromatography A* **2003**, *983* (1), 237−246.
(69) Rowdhwal, S. S. S.; Chen, J. Toxic Effects of Di-2-Ethylhexyl Phthalate: An Overview. *Biomed Res. Int.* **2018**, *2018*, No. 1750368.
(70) Koniecki, D.; Wang, R.; Moody, R. P.; Zhu, J. Phthalates in Cosmetic and Personal Care Products: Concentrations and Possible Dermal Exposure. *Environmental Research* **2011**, *111* (3), 329−336.
(71) Djapovic, M.; Milivojevic, D.; Ilic-Tomic, T.; Lješević, M.; Nikolaivits, E.; Topakas, E.; Maslak, V.; Nikodinovic-Runic, J. Synthesis and Characterization of Polyethylene Terephthalate (PET) Precursors and Potential Degradation Products: Toxicity Study and Application in Discovery of Novel PETases. *Chemosphere* **2021**, *275*, No. 130005.
(72) Kleindienst, T. E.; Jaoui, M.; Lewandowski, M.; Offenberg, J. H.; Docherty, K. S. The Formation of SOA and Chemical Tracer Compounds from the Photooxidation of Naphthalene and Its Methyl Analogs in the Presence and Absence of Nitrogen Oxides. *Atmospheric Chemistry and Physics* **2012**, *12* (18), 8711−8726.
(73) Lewis, R. J., Sr. *Hawley's Condensed Chemical Dictionary*, 15th ed.; John Wiley & Sons, Inc.: New York, NY, 2007.
(74) O'Neil, M. J. *The Merck Index : An Encyclopedia of Chemicals, Drugs, and Biologicals*, 15th ed.; Royal Society of Chemistry : Cambridge, UK, 2013.
(75) Schmiedel, K. W.; Decker, D. *Ullmann's Encyclopedia of Industrial Chemistry*, 7th ed.; John Wiley & Sons, Inc.: New York, NY, 2011.
(76) Hiroshi, O.; Kazuyoshi, O.; Go, O.; Iho, K. Epoxy Resin Composition, Curable Resin Composition, Cured Product, and Adhesive. WO-2020213642-A1. https://pubchem.ncbi.nlm.nih.gov/patent/WO-2020213642-A1 (accessed 2024-07-17).
(77) Van der Steen, M.; Stevens, C. V. Undecylenic Acid: A Valuable and Physiologically Active Renewable Building Block from Castor Oil. *ChemSusChem* **2009**, *2* (8), 692−713.
(78) Crocker, G. J.; Doehnert, D. F. Modified Acrylate Adhesive Product. US-3551391-A, 1968. https://pubchem.ncbi.nlm.nih.gov/patent/US-3551391-A (accessed 2024-07-17).
(79) Keika, H.; Yuki, M.; Masao, T. Resin Composition, Resin Sheet, Cured Film, Method for Manufacturing Cured Film, Semiconductor Device, Organic El Display Device, and Display Device. WO-2021085321-A1, 2019. https://pubchem.ncbi.nlm.nih.gov/patent/WO-2021085321-A1 (accessed 2024-07−-17).

https://doi.org/10.1021/acsestair.4c00215
ACS EST Air 2024, 1, 1495−1506

(80) Kazuko, N.; Shigeki, K. Metal Pigment Composition. EP-2093262-A1, 2006. https://pubchem.ncbi.nlm.nih.gov/patent/EP-2093262-A1 (accessed 2024-07-17).
(81) Koji, F.; Atsuhito, A.; Hiroaki, S. Epoxy Resin Composition, Prepreg, Cured Resin, and Fiber Reinforced Composite Material (as Amended). US-10351700-B2, 2019. https://pubchem.ncbi.nlm.nih.gov/patent/US-10351700-B2 (accessed 2024-07-17).

https://doi.org/10.1021/acsestair.4c00215
ACS EST Air 2024, 1, 1495−1506